Effect of Diisocyanate Structure on the Properties and Microstructure of Polyurethanes Based on Polyols Derived from Renewable Resources

Ma. Angeles Corcuera, Lorena Rueda, Ainara Saralegui, Ma. Dolores Martín, Borja Fernández-d'Arlas, Iñaki Mondragon, Arantxa Eceiza

Materials and Technologies Group, Department of Chemical and Environmental Engineering, Polytechnic School, University of the Basque Country, Pza Europa 1, 20018, Donostia-San Sebastián, Spain

Received 28 April 2011; accepted 28 April 2011
DOI 10.1002/app.34781
Published online 11 August 2011 in Wiley Online Library (wileyonlinelibrary.com).

ABSTRACT: Polyols derived from renewable resources are good candidates for obtaining segmented polyurethane (PU) elastomers. Diisocyanates with different chemical structures, aliphatic and aromatic, were used to synthesize PU elastomers with different hard-segment (HS) contents by a two-step polymerization procedure. Microphase separation and thermal stability were studied with attenuated total reflection Fourier transform infrared spectroscopy, differential scanning calorimetry, and thermogravimetric analysis. The analysis of H-bonded and non-H-bonded urethane carbonyl stretching vibration in the amide I region, the glass-transition temperatures of the soft segments and HSs, and the melting temperature and enthalpies of the HSs revealed that aliphatic diisocyanate based PUs presented a higher phase separation degree and higher HS crystallinity and also a superior thermal stability to the aromatic diisocyanate-based PUs. The aromatic diisocyanate-based PU presented a higher ductility, higher tensile strength, and lower modulus than aliphatic diisocyanate-based PU for the same HS content because of the different morphology that they presented. © 2011 Wiley Periodicals, Inc. J Appl Polym Sci 122: 3677–3685, 2011

Key words: elastomers; polyurethane; structure; thermal properties

INTRODUCTION

Polyols derived from vegetable oils are new materials from renewable sources.[1,2] Combined with diisocyanates, these polyols produce polyurethanes (PUs) that can compete in many aspects with PUs derived from petrochemical polyols and reduce the environmental impact. These PU can be used in many applications, such as abrasion-resistant components, biomaterials, durable coatings, and foams.[3,4] Segmented PU elastomers are block copolymers formed by soft segments (SS) and hard segments (HS). The SS, formed by the polyol, provides extensibility, and the HS, formed by the diisocyanate and chain extender, plays the role of a physical crosslinker and acts as a high-modulus filler. The incompatibility between both segments causes phase separation determined by factors such as the chemical structure of the PU precursors, segmental lengths, nature of the interfacial region between the segments, hydrogen bonding (intermolecular and intramolecular interactions), and crystallization extent.[5] The nature of hydrogen bonding in the HS causes a strong mutual attraction, which leads to hard- and soft-domain formation.[6,7] The interesting properties of segmented PU elastomers are strongly dependent on their phase-separated morphologies.[8]

The choice of monomers used to synthesize elastomeric PUs is dependent on the final applications of the material. It is well known that the properties of PUs are remarkably affected by the content, type, and molecular weight of the SS.[5,9] The nature of diisocyanate also concerns the PU properties.[5,10,11] The study of the effects of the diisocyanate structure on the microstructure and thermal and mechanical properties was the main aim of this work.

This work was focused on the development of segmented PUs based on polyols derived from renewable sources because they can be potential candidates to replace or partially replace petroleum-based PUs in the market.

Segmented PU elastomers based on castor oil as the SS were synthesized with 1,4-butanediol (BD) as a chain extender and two diisocyanates, one aliphatic, 1,6-hexamethylene diisocyanate (HDI), and the other aromatic, 4,4′-diphenylmethane diisocyanate (MDI), as components of the HS by a two-step synthetic procedure. The microphase structure and

Correspondence to: A. Eceiza (arantxa.eceiza@ehu.es).
Contract grant sponsor: Gobierno Vasco Saiotek; contract grant number: S-PE09UN07 and S-PE10UN22.
Contract grant sponsor: Grupos de Investigación Consolidados; contract grant number: IT-365-07.

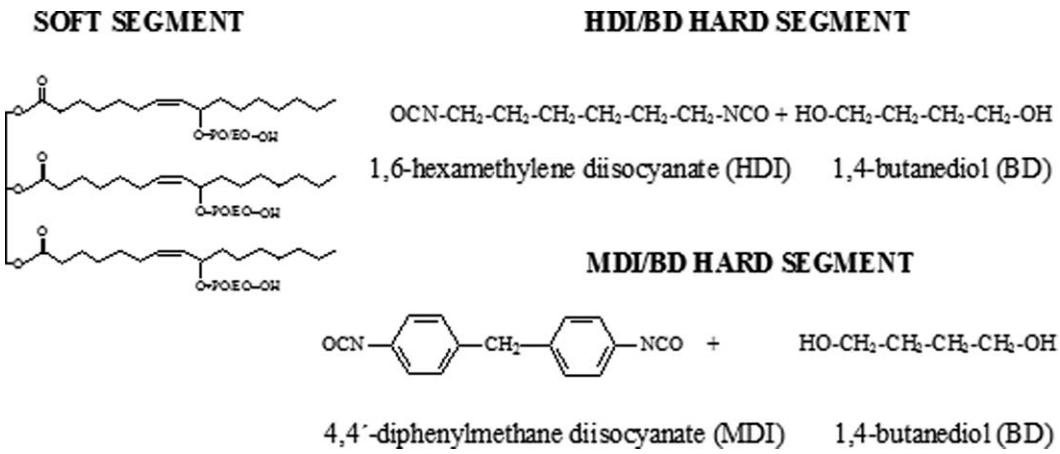

Figure 1 Chemical structure of SS and HS of synthesized PUs.

properties were analyzed with attenuated total reflection Fourier transform infrared (ATR-FTIR) spectroscopy and differential scanning calorimetry (DSC) as complementary techniques to characterize the PU thermal transitions and relate them to interactions between functional groups. Measurements of the tensile properties and Shore D hardness were performed, and the results obtained were related with the different morphologies of the synthesized PU systems. The thermal stability was also analyzed by means of thermogravimetric analysis (TGA).

EXPERIMENTAL

Raw materials

Segmented PU elastomers were synthesized with HDI (Desmodur H) or MDI (Desmodur 44), which were kindly provided by Bayer (Leverkusen, Germany); a castor-oil-derived polyol, (Lupranol Balance 50) kindly supplied by BASF (Lemförde, Germany); and BD as chain extender, which was provided by Aldrich. The polyol number-average molecular weight was 3366 g/mol, as determined with ASTM D 4274-88 for measuring the hydroxyl number. Before use, the polyol and BD were dried *under vacuum* for 12 h at 90 and 40°C, respectively. HDI and MDI were used as received. The chemical structures of the polyol, diisocyanates, and chain extender are shown in Figure 1.

Synthesis of the PUs

The PUs were synthesized with a two-step bulk polymerization procedure (Scheme 1). All PUs were prepared by the reaction of equimolar amounts of isocyanate groups and hydroxyl groups. Dried polyol and an excess of diisocyanate were placed in a three-necked round-bottom flask fitted with a dry nitrogen inlet, condenser, and mechanical stirrer and heated in a thermoregulated silicon bath for 5 h at 90°C for the HDI-based system (designated as PUHDI) and 5 h at 80°C for the MDI-based system (designated as PUMDI) according to kinetics measurements, with stirring to end-cap the macrodiol with diisocyanate. The chain extender was added to the prepolymer at 90°C for the PUHDI system and at 60°C for the PUMDI system with rapid stirring with a stainless steel paddle for 10 min to homogenize the mixture and to evacuate the air trapped within it.[12] The resulting viscous liquid was quickly poured between two Teflon-coated metal plaques separated by 1.5 mm and left to cure under pressure for 10 h at 100°C. The PUs were designed as listed in Table I.

Characterization techniques

Infrared spectroscopy

ATR–FTIR spectroscopy was used to characterize the functional groups of the synthesized PUs and also to investigate hydrogen-bonding formation in the HS. Measurements were performed with a Nicolet Nexus FTIR spectrometer (Madison, WI) equipped with a MKII Golden Gate accessory, Specac (Kent, United Kingdom), with diamond crystal as the ATR element at a nominal incidence angle of 45° with a ZnSe lens. Single-beam spectra of the samples were obtained after averaging 20 scans in the range from 4000 to 600 cm^{-1} with a resolution of 2 cm^{-1}.

DSC

DSC thermograms in the low-temperature behavior of the synthesized PUs were obtained by cooling the sample from room temperature to −90°C with an intracooler and then heating it up to 0°C at 20°C/min under a dry helium atmosphere with a Perkin-Elmer DSC-7 instrument (Norwalk, CA). The thermal behavior above room temperature of the PUMDI and PUHDI PU systems was investigated by scanning the specimens from −60 up to 200°C under a dry nitrogen atmosphere at a scan rate of 20°C/min. The sample weights employed were 5–10 mg.

The midpoint of the heat capacity change was chosen to represent the glass-transition temperature.

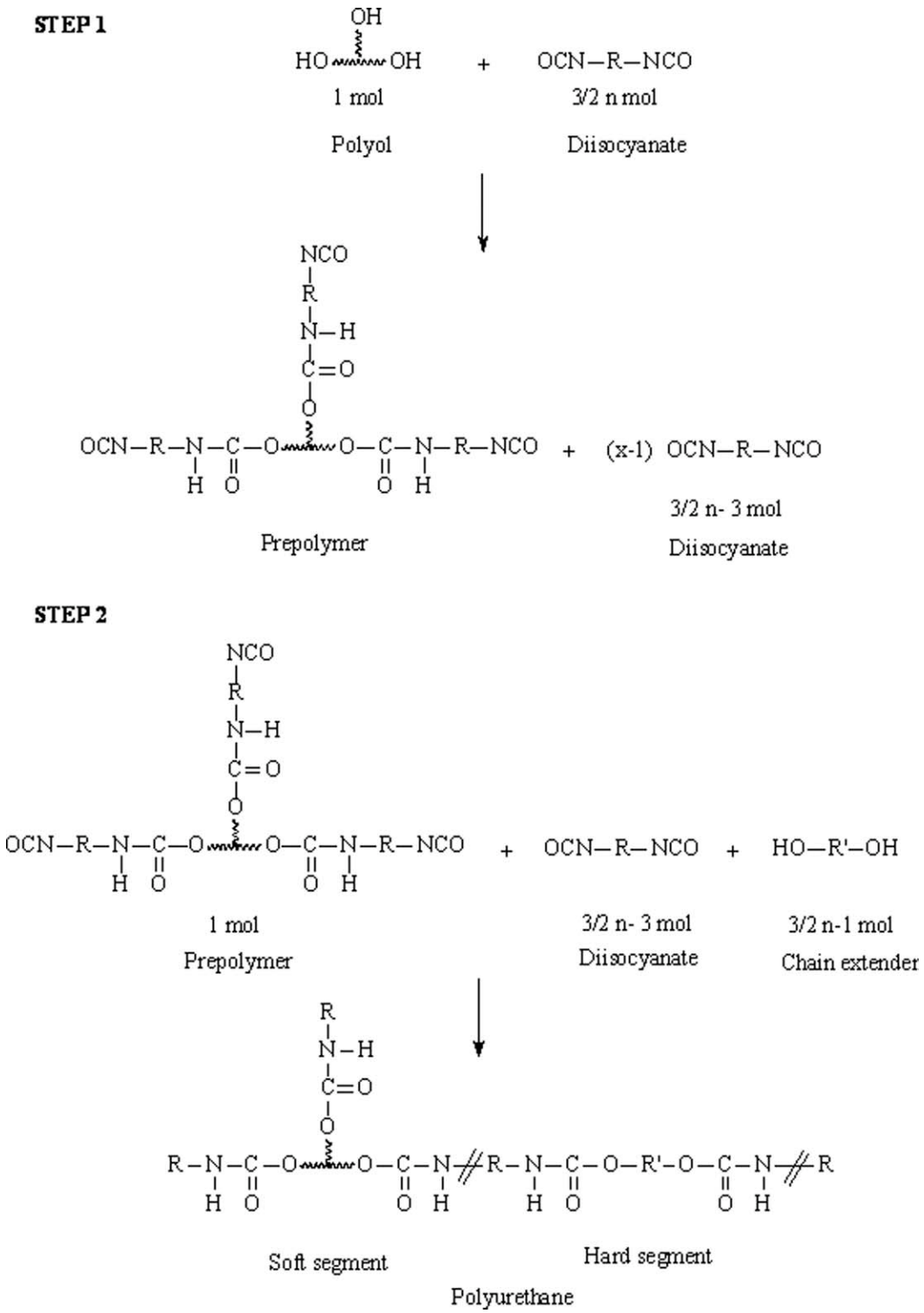

Scheme 1 Reaction steps for the synthesis of the PUs.

The melting temperatures (T_m's) refer to the maximum of the endotherm peak temperatures.

TGA

TGA at a scanning rate of 10°C/min from room temperature up to 700°C under a nitrogen atmosphere was performed to investigate the PU thermal stability with a Mettler-Toledo TGA/SDTA 851.

Water contact angle

Water contact angle measurements were carried out in a Dataphysics OCA20 to evaluate the surface

TABLE I
Molar Ratio, HS Content, and Designation of the Synthesized PUs

PU	Molar ratio of polyol to diisocyanate to chain extender	HS (wt %)
PUHDI-1	1 : 3 :2	21
PUHDI-2	1 : 5 : 4	32
PUHDI-3	1 : 7 : 6	40
PUHDI-4	1 : 11 : 10	50
HDI/BD	0 : 1 : 1	100
PUMDI-1	1 : 3 : 2	27
PUMDI-2	1 : 5 : 4	39
PUMDI-3	1 : 7 : 6	48
PUMDI-4	1 : 11 : 10	59
MDI/BD	0 : 1 : 1	100

properties. Six measurements of each sample of the different PU systems were carried out with a deionized water drop method (2 μL) at 26°C.

Mechanical behavior

Samples for mechanical behavior analysis were cut into dog-bone shapes with a thickness of 1.5 mm according to ASTM D 1708-93. MTS equipment (Glos, United Kingdom) with a load cell of 250 N and pneumatic grips were used to measure the modulus of elasticity, tensile strength at break, and percentage elongation at break. Tests were performed with a crosshead rate of 100 mm/min. Tensile properties were averaged for at least five specimens. The PU systems' hardness was also analyzed. An MD-202 DuroTECH machine (Northampton, England) was used to evaluate the Shore D hardness according to ASTM D 2240-86/DIN 53505. The final result was the average of five measurements taken in different parts of the sample.

RESULTS AND DISCUSSION

ATR–FTIR spectroscopy was used to investigate the effect of the HDI and MDI diisocyanate chemical structure and HS content on the microstructure of the PUs by means of hydrogen-bonding formation in the amide I region. Figure 2(a–c) shows typical infrared spectra of the HDI- and MDI-based PUs and also pure polyol. Polyol showed a broad hydroxyl band between 3680 and 3290 cm^{-1} and a characteristic triglyceride ester carbonyl band at 1743 cm^{-1}. Moreover, all of the spectra of each synthesized PU system were similar, and they did not show the stretching vibration band at 2270 cm^{-1} characteristic of the isocyanate (—N=C=O) group, which confirmed that all of the isocyanate groups reacted during the polymerization.

It is well known that the infrared absorbance of H-bonded urethane carbonyl groups in ordered (crystalline) hard domains appears at lower wave number than that of H-bonded urethane carbonyl

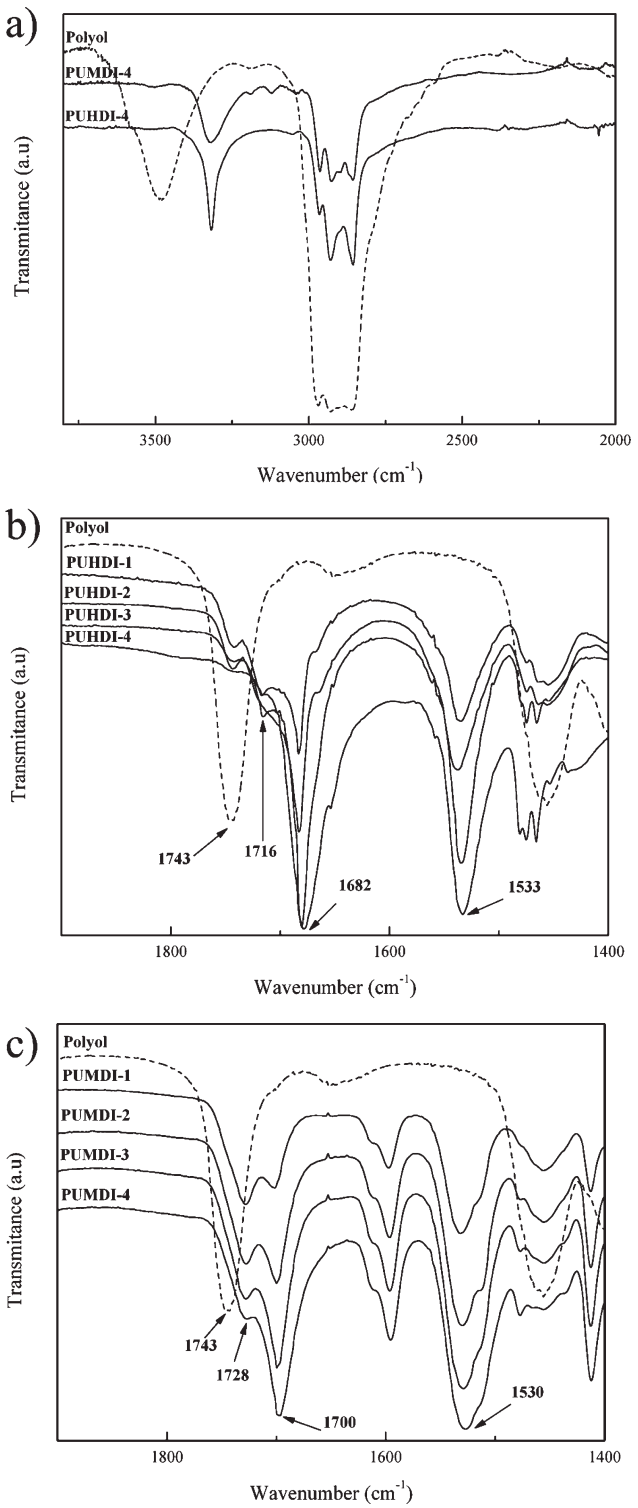

Figure 2 ATR–FTIR spectra of (a) the pure polyol and PU systems, (b) the stretching vibration carbonyl group region in the PUHDI system, and (c) the stretching vibration carbonyl group region in PUMDI systems.

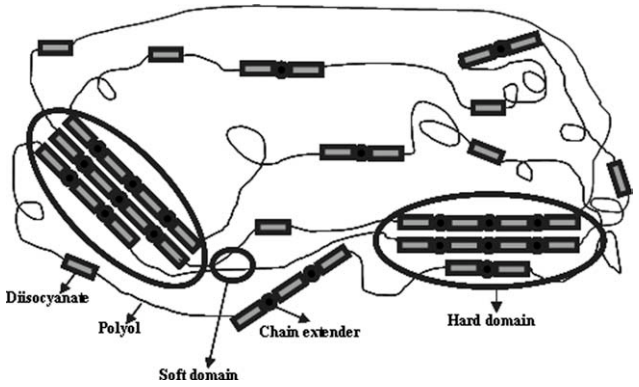

Scheme 2 Schematic representation of microstructure of segmented elastomeric PUs showing hard and soft microdomains.

groups in disordered (amorphous) domains.[6,13] On the other hand, the urethane carbonyl band appears at different wave number, depending on whether the free electron pair of the amine group is conjugated with the π bond of the carbonyl group in HDI-based PUs or with the aromatic ring in MDI-based PUs. In both PU systems, although the bands associated with H-bonded urethane carbonyl groups in disordered domains at 1728 and 1716 cm^{-1} for the MDI- and HDI-based PUs, respectively, decreased with increasing HS content, the H-bonded urethane carbonyl groups in ordered hard domains at 1700 and 1682 cm^{-1} for the MDI- and HDI-based PUs, respectively, increased with increasing HS content. In this way, it provoked the formation of large HS domains that contributed to the phase-separated microstructure (Scheme 2). The relative intensity of H-bonded urethane carbonyl groups in disordered hard domains with respect to H-bonded urethane carbonyl groups in ordered hard domains was higher for the MDI-based PU, which could have indicated that a less phase-separated microstructure was obtained. In this way, the band associated with the polyol carbonyl group in the MDI-based PUs was not observed, as it could be masked with the H-bonded urethane carbonyl groups in disordered domains. The higher intensity observed for the H-bonded urethane carbonyl groups in ordered hard domains for HDI-based PUs could be related with a higher hard-domain crystallinity degree by means of H-bonding formation.

On the other hand, the stretching vibration combined with out-of-the plane bending at 1530–1533 cm^{-1}, amide II, characteristic of C—N bonds in urethane group, increased with the HS content for both synthesized PU systems.

As can be seen in Figure 2(a–c), where the spectra of the HDI and MDI PU systems are shown together with the polyol spectra, the absorption bands related to the covalent bonds involved in urethane groups, such as amide I and amide II bands, and the stretching vibrations of —NH at 3400–3200 cm^{-1}, of the PUHDI system were sharper than those of the PUMDI system. This fact was related to the higher distribution of hydrogen-bonded species as a consequence of the poorer phase segregation of the MDI-based HS compared to the HDI-based ones.

Segmented PUs typically display several thermal transitions that could be related to microdomain purity or microdomain separation degree, that is, the presence of HS in the soft domain and vice versa. The soft domains possessed a low-temperature glass transition and a melting transition when semicrystalline; the hard domains may also have had a glass transition and/or multiple melting transitions because of the distribution of HS lengths. The soft- and hard-domain thermal transitions of the PUHDI and PUMDI systems were investigated by means of DSC (Fig. 3). The measured values are given in Table II. The soft-segment glass-transition temperature (T_{gSS}) values around −51 and −42°C for the PUHDI and PUMDI systems, respectively, were higher than the value measured for pure polyol, which showed a T_{gSS} value of −62.8°C. This could have been indicative of the chain extension occurring during the first step of the polymerization and also of the HS dissolved into the soft domain. However, the almost constant T_{gSS} observed in both analyzed systems, that is, independent of the HS content, denoted that mixing between HS and SS did not depend on the excess of diisocyanate in the polymerization first step. Similar results were reported in polyether diol SS-based PUs.[14,15]

In the high-temperature behavior, different transitions associated with HS were observed. The hard-segment glass-transition temperature (T_{gHS}) showed values around 50 and 62°C for the PUHDI and PUMDI systems, respectively, being 52 and 100°C for HDI/BD and MDI/BD pure HS, respectively. T_{gHS} remained nearly constant as the HS content increased; this fact seemed to indicate that the mixing degree between SS and HS was independent of HS content, as also observed in T_{gSS}. The results obtained show that the T_{gSS} and T_{gHS} values of the PUHDI systems were closer to the T_{gSS} and T_{gHS} values of pure SS and HS; this indicated that the PUHDI systems were more phase-separated than the PUMDI systems, which suggested that mixing between segments was relatively low. These results were in agreement with the results obtained by FTIR spectroscopy.

On the other hand, the hard-segment melting temperatures (T_{mHS}) of both PU systems increased with increasing HS content because of the increment in the average molecular weight of crystallizable HS and the ability of segments to form more interurethane interactions. Although the MDI-based PU systems showed higher T_m's, lower values of the melting enthalpies (ΔH_m's) were measured; this

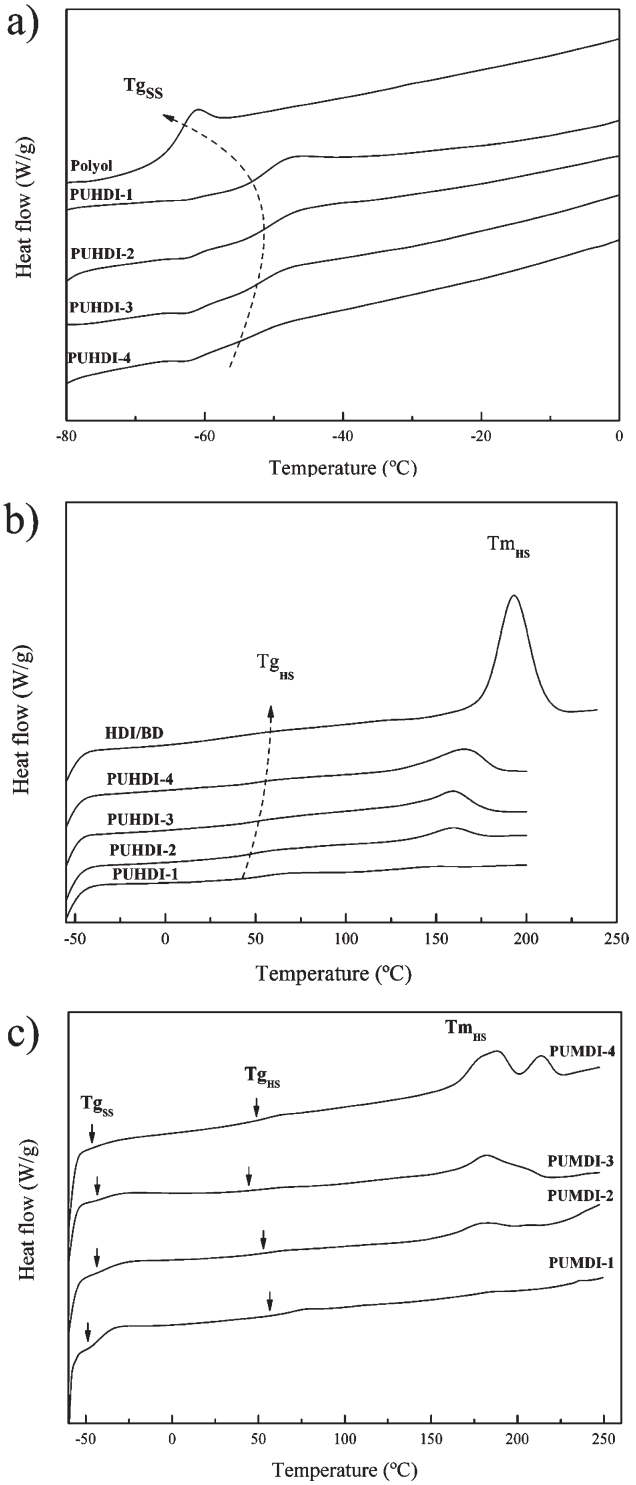

Figure 3 DSC thermograms of the (a) low-temperature behavior of the PUHDI systems, (b) high-temperature behavior of the PUHDI systems, (c) low- and high-temperature behavior of the PUMDI systems.

indicated that this system was less able to crystallize, which could have been related to the steric hindrance that the aromatic ring introduced into the HS structure, which lowered hydrogen-bonding formation, as shown previously by FTIR spectroscopy. The existence of broader and several endotherms in the PUMDI system was related to higher hydrogen-bonding species distribution due to the poorer phase segregation of the MDI-based HS.

TABLE II
Thermal Properties of the Pure Polyol, Pure HS, and PU Systems

PU	T_{gSS} (°C)	T_{gHS} (°C)	T_m (°C)	ΔH_m (J/g)
Polyol	−62.8	—	—	—
PUHDI-1	−50.1	58.2	149.9	3.1
PUHDI-2	−50.9	53.7	158.8	13.2
PUHDI-3	−50.9	46.7	159.8	27.9
PUHDI-4	−51.2	50.2	164.1	40.8
HDI/BD	—	52.1	189.0	122.3
PUMDI-1	−42.1	69.8	176.7	0.9
PUMDI-2	−42.7	62.2	181.2/205.3	7.6
PUMDI-3	−41.8	58.8	182.4/206.4	15.3
PUMDI-4	−42.1	62.2	187.8/214.5	26.7
MDI/BD	—	100.0	199.5/220.4	39.6

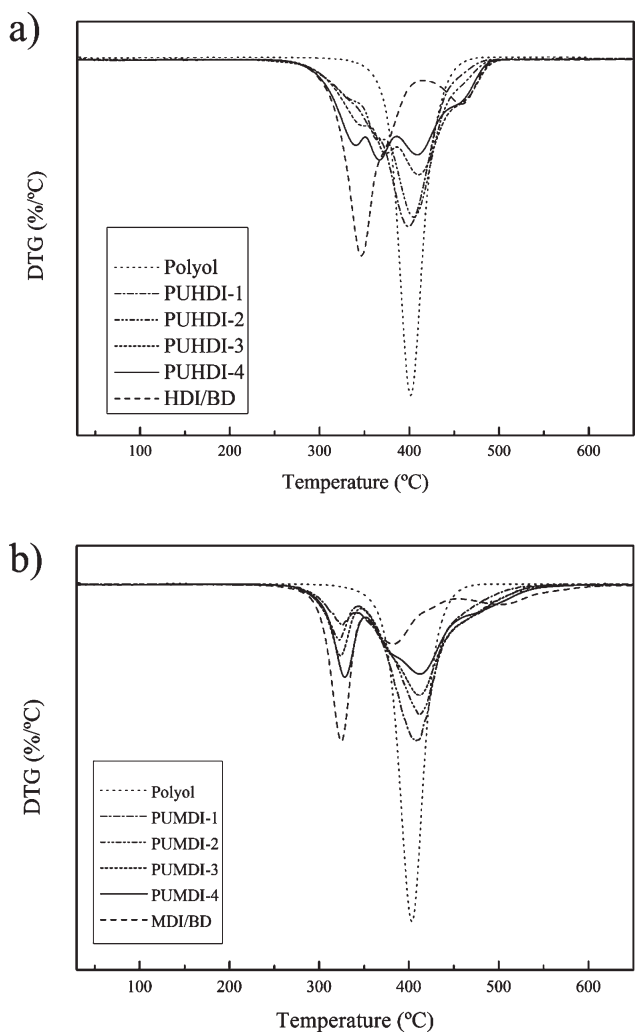

Figure 4 Derivate of weigh loss for the (a) pure polyol and PUHDI systems and (b) pure polyol and PUMDI systems.

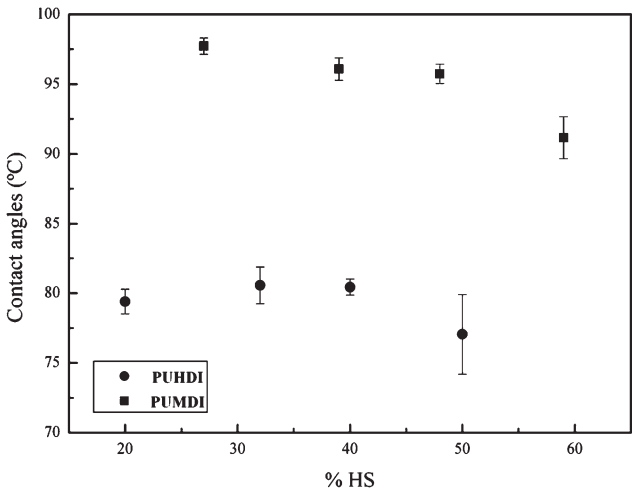

Figure 5 Contact angle values of the PUHDI and PUMDI systems with different HS contents.

The thermal degradation of PUs, attributed to absorbed thermal energy, is a complex heterogeneous process and consists of several partial decomposition reactions.[16] The degradation of PUs occurs as a result of a multitude of physical and chemical phenomena and is not dominated by a single process. The study of the degradation of PUs is particularly difficult because they degrade with the formation of various gaseous products, and a number of decomposition stages are typically observed in TGA experiments. In this work, TGA was used to study the thermal degradation of the synthesized PUs. Normally, thermal degradation of PU occurs in a two- to three-stage process.[17–19] The first stage is due to the urethane bond decomposition, which results in the formation of isocyanate and alcohol, primary or secondary amine and olefin, and carbon dioxide. The rate of the first degradation stage decreases with the increase of SS content. The second and third stages correspond to the SS thermal decomposition and depend on the SS structure and its three-dimensional arrangement. The temperature at which the urethane bond degradation starts depends on the structure of the isocyanate and alcohol. PUs based on alkyl diisocyanates show a higher thermal stability than PUs based on aryl diisocyanates.[17,20] Figure 4 presents the thermal degradation behavior of the PUHDI and PUMDI systems with different HS contents. Even though both PU systems showed similar second and third degradation stages, differences in the first degradation stage were observed. Indeed, the MDI-based PU showed a first degradation stage between 260 and 345°C, and HDI-based PU showed a first degradation stage between 270 and 370°C. The increase of amorphous HS content inside the HS domain, due to the lower crystallinity degree observed for PUMDI systems, constituted a weak point inside the HS domain, which therefore, degraded at lower temperature. As observed, PU based on HDI presented a higher thermal stability than PU based on MDI. For both PU systems, an increase of HS content, that is, a higher urethane group concentration, resulted in a lower thermal stability.

Thermal stability is a key factor and determines the final applications of PU. The stability observed for the PUHDI and PUMDI systems prepared in this work was comparable to that observed for PU based on polyols derived from petroleum;[8,21] this indicated that polyols derived from renewable sources are good candidates for the synthesis of PU with a high content of renewable carbon.

Contact angle analysis provides information on the surface hydrophobicity or hydrophilicity and molecular mobility at the air–water–solid interface.[22] High contact angle values, included between 100 and 110°, are typical of surfaces with high hydrophobicity, such as silicone or fluorocarbon polymers,[23] whereas low contact angle values (0–30°) are typical of highly hydrophilic surfaces, such as glass

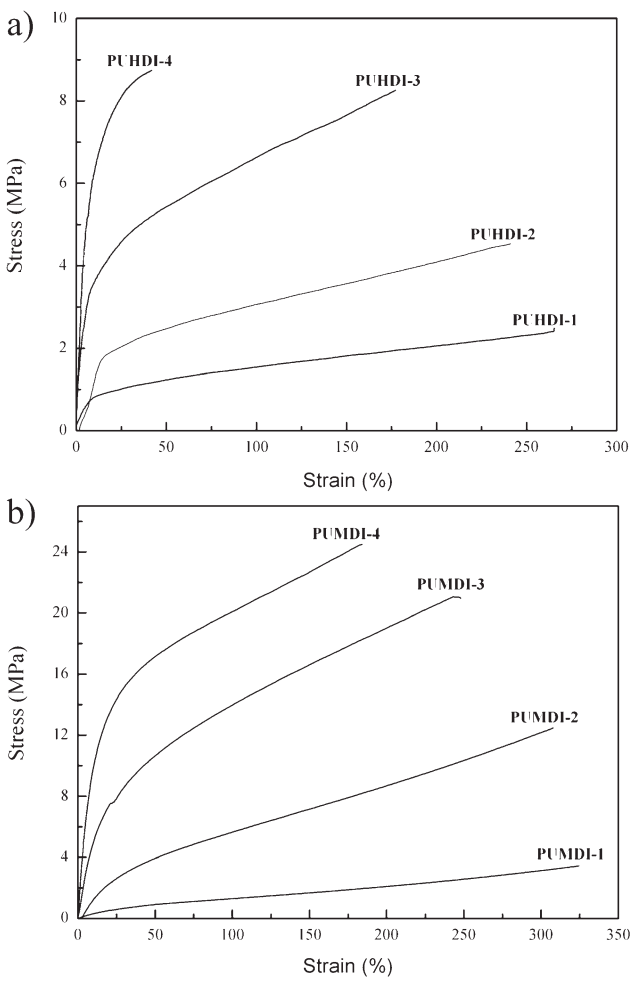

Figure 6 Stress–strain curves of the (a) PUHDI and (b) PUMDI systems with various HS contents.

TABLE III
Mechanical Properties of the PU Systems: Tensile Strength, Elongation at Break, Modulus of Elasticity, and Shore D Hardness

PU	Tensile strength (MPa)	Elongation at break (%)	Modulus of elasticity (MPa)	Shore D hardness
PUHDI-1	2.90 ± 0.4	260.67 ± 52.43	11 ± 0.72	18.21 ± 0.57
PUHDI-2	3.98 ± 0.49	237.97 ± 36.91	27.88 ± 3.05	22.65 ± 1.22
PUHDI-3	8.57 ± 0.57	193.56 ± 29.47	68.53 ± 18.91	37.18 ± 2.16
PUHDI-4	8.25 ± 0.94	49.26 ± 5.35	95.85 ± 31.45	43.65 ± 1.81
PUMDI-1	3.19 ± 0.13	305.33 ± 23.70	2.87 ± 0.18	17.56 ± 0.21
PUMDI-2	12.49 ± 0.28	265.51 ± 29.76	15.14 ± 3.79	33.68 ± 1.59
PUMDI-3	22.27 ± 2.10	241.54 ± 35.41	56.35 ± 2.96	40.52 ± 1.80
PUMDI-4	23.84 ± 1.03	178.05 ± 23.38	142.85 ± 5.23	57.54 ± 1.60

or mica.[24] The hydrophobicity or hydrophilicity of PU systems can be characterized by contact angle.

Figure 5 shows the contact angles for both PU systems as a function of HS content. It is worth noting that the MDI-based PUs presented higher contact angles values than the HDI-based ones; this meant a lower hydrophilicity or polarity. These results could have been due to the markedly difference in phase-separation behavior; because the PUs microdomains considered as electric dipoles, it was clear that MDI-based PUs, poorly phase-separated, would have led to few and smaller dipoles, which would provide the materials with a more hydrophobic character. These results were in agreement with the results obtained by other techniques.

Figure 6 gathers some representative curves of tensile tests results from both the PUHDI and PUMDI systems. Tensile properties, such as the percentage elongation at break, tensile strength, and modulus of elasticity, measured by stress–strain uniaxial tests are listed in Table III. As observed for both of the analyzed PU systems, as the HS content increased, the modulus of elasticity and tensile strength increased, but the elongation at break decreased. As seen, MDI-based PUs presented a higher ductility, higher tensile strength, and lower modulus than the HDI-based PUs for the same HS content. This was related to the differences previously observed in the phase morphology. The much higher tensile strength of MDI-based PUs should have been due to the less phase-separated structure, which could have given place to an orientation of the hard domains during the strain. In the case of the HDI-based PUs, the highly crystalline structure of hard domains must have had a hindrance effect over the whole PU network and prevented the hard domains from dispersing into soft phases to give a strain-induced crystallization phenomena.[25]

The different PU microstructures and natures also had an effect on their macroscopic behavior, which was reflected in their hardness. The Shore D hardness of both the PUHDI and PUMDI systems (Table III) increased as the HS content increased. On the other hand, the PUHDI PUs were harder than those based on MDI for the whole composition range studied. The higher the hydrogen bonding and phase separation were among the materials, the harder the material was. These results were also in agreement with the modulus of elasticity and contact angle results.

CONCLUSIONS

Two series of different diisocyanate chemical structure based PUs (PUHDI and PUMDI) with different HS contents were synthesized via a two-step bulk polymerization. The effect of HS structure and content on phase separation was investigated by ATR–FTIR spectroscopy and DSC.

The FTIR and DSC results showed that the PUHDI systems presented less distribution of hydrogen-bonded species and gave a more phase-separated and crystalline HS morphology in comparison to those based on PUMDI. T_{gSS} and T_{gHS} revealed that the phase separation in both the PUHDI and PUMDI systems was independent of HS content. T_m's and enthalpies increased with the HS content, that is, the urethane units involved in the HS. The thermal decomposition mechanism followed the same behavior in both of the synthesized PU series. With the segmented structure observed for the synthesized PUs taken into account, the degradation process occurred mainly in two events, which consisted of HS and SS degradation, respectively. In this way, an increase in hydrogen-bond interaction in the HS and, as a consequence, crystallinity, led to a higher thermal stability.

PUs with HS based on HDI presented a higher modulus of elasticity and higher hardness but a lower elongation at break and tensile strength than those based on MDI; this suggested a more severe strain-induced crystallization of HS in the case of MDI-based PUs than in the case of the more crystalline HDI analogues.

The authors thank General Research Services (SGIker)-Nano/Mesostructure Group from the Research Services from the University of the Basque Country.

References

1. Williams, C. K.; Hillmyer, M. A. Polym Rev 2008, 48, 1.
2. Gandini, A. Macromolecules 2008, 41, 9491.
3. Uyama, H.; Kuwabara, M.; Kobayashi, S. Biomacromolecules 2003, 4, 211.
4. Krol, P.; Pilch-Pitera, B. Eur Polym J 2001, 37, 251.
5. Yilgor, I.; Yilgor, E.; Guler, I. G.; Ward, T. C.; Wilkes, G. L. Polymer 2006, 47, 4105.
6. Coleman, M. M.; Lee, K. H.; Skrovanek, D. J.; Painter, P. C. Macromolecules 1986, 19, 2149.
7. Ning, L.; De-Ning, W.; Shenk-Kang, Y. Macromolecules 1997, 30, 4405.
8. Rueda-Larraz, L.; Fernandez d'Arlas, B.; Tercjak, A.; Ribes, A.; Mondragon, I.; Eceiza, A. Eur Polym J. 2009, 45, 2096.
9. Korley, L. T. J.; Pate, B. D.; Thomas, E. L.; Hammond, P. T. Polymer 2006, 47, 3076.
10. Fernández d'Arlas, B.; Rueda, L.; de la Caba, K.; Mondragon, I.; Eceiza, A. Polym Eng Sci 2008, 48, 519.
11. Kojio, K.; Nakashima, S.; Furukawa, M. Polymer 2002, 3, 153.
12. Fernández d'Arlas, B.; Rueda, L.; Stefani, P. M.; de la Caba, K.; Mondragon, I.; Eceiza, A. Thermochim Acta 2007, 459, 94.
13. Sormana, J. L.; Meredith, J. C. Macromolecules 2004, 37, 2186.
14. Paik Sung, C. S.; Hu, C. B.; Chu, B. Macromolecules 1993, 26, 612.
15. O'sickey, M. J.; Lawrey, B. D.; Wilkes, G. L. J Appl Polym Sci 2002, 84, 229.
16. Scaiano, J. C.; Laser Photolysis in Polymer Chemistry. Degradation and Stabilization of Polymers; Elsevier: Amsterdam, 1989.
17. Petrovic, Z. S.; Zavargo, Z.; Flynn, T.; Macknight, W. J. J Appl Polym Sci 1994, 51, 1087.
18. Javni, I.; Petrovic, Z. S.; Guo, A.; Fuller, V. J Appl Polym Sci 1999, 77, 1723.
19. Lage, L. G.; Kawano, Y. J Appl Polym Sci 2001, 79, 910.
20. Song, Y. M.; Chen, W. C.; Yu, T. L.; Linliu, K.; Tseng, Y. H. J Appl Polym Sci 1996, 62, 827.
21. Chuang, F. S. Polym Degrad Stab 2007, 92, 1393.
22. Andrade, J. D.; Smith, L. M.; Grenois, D. E. Interfacial Aspect of Biomedical Polymer. I. Surface Chemistry and Physics; Plenum: New York, 1985.
23. Iwanori, S.; Hasegawa, Uemura, A. Surf Coat Technol 2008, 203, 59.
24. Good, R. J. Contact Angle, Wettability and Adhesion; VSP: Utrecht, The Netherlands, 1993.
25. Williams, S. R.; Wang, W.; Winey, K. I.; Long, T. E. Macromolecules 2008, 41, 9072.